analytical chemistry

pubs.acs.org/ac Article

Rapid and Sensitive Pathogen Detection by DNA Amplification Using Janus Particle-Enabled Rotational Diffusometry

Dhrubajyoti Das, Wei-Long Chen, and Han-Sheng Chuang*

Cite This: https://doi.org/10.1021/acs.analchem.1c03209 Read Online

ACCESS | Metrics & More | Article Recommendations | Supporting Information

Downloaded via NATL CHENG KUNG UNIV on October 8, 2021 at 00:30:46 (UTC).
See https://pubs.acs.org/sharingguidelines for options on how to legitimately share published articles.

ABSTRACT: Rapid and sensitive detection of infectious bacteria is in all-time high demand to prevent the further spread of the infection and allow early medical intervention. In this study, we use rotational diffusometry (RD), a natural phenomenon characterized by Janus particles, to detect pathogens like *Escherichia coli* by performing amplification of specific genes. This biosensing method is used to measure the change in viscosity of the fluid in the presence and absence of DNA in the solution by capturing images of modified microbeads at 10 Hz by a CCD camera followed by cross-correlation algorithm analysis. Using rotational diffusometry, we have achieved *E. coli* detection with 50 pg/μL DNA with a measurement time of 30 s and a sample volume of 2 μL. This sensitivity was achieved with 30 thermal cycles for three different amplicons, *viz.*, 84, 147, and 246 bp. Meanwhile, in the case of 10 and 20 thermal cycles, the detection sensitivity was achieved with 0.1 and 1 ng/μL DNA concentrations for a 246 bp amplicon. Compared with conventional PCR, this technique appears to improve the detection time, thereby reaching a turnaround time of less than 60 min. Other studies showed a successful identification of DNA amplification up to 10 thermal cycles with different sizes of amplicons. The effect of DNA concentration, amplicon size, and the number of thermal cycles on the detection of *E. coli* was examined in detail and represented in the form of three maps. These maps show the clear difference and the advantages of RD method in comparison with conventional PCR. This unconventional and rapid biosensing method can be used further for downstream application of nucleic acid amplification-based pathogen detection and early disease control.

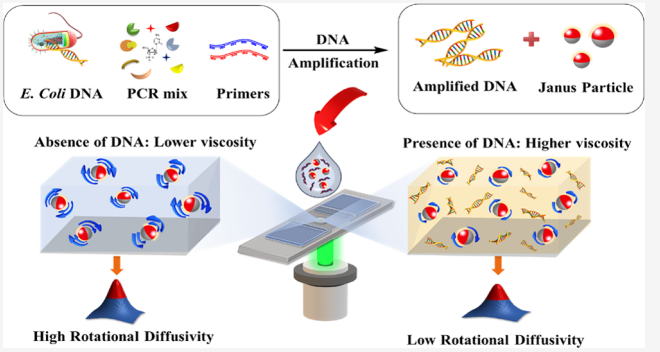

Pathogenic bacterial infections result in millions of deaths and hospitalizations annually throughout the world. Among the various bacterial strains, *Escherichia coli* is one of the most hazardous pathogens, posing a serious threat to humans.[1−4] Therefore, it is significantly important to develop a fast, sensitive, and specific detection method to provide the best suitable treatment and to prevent the spread of infections further. Traditional detection methods like microbial culture are widely used but consume a lot of time and labor.[5,6] As an alternative, the enzyme-linked immunosorbent assay (ELISA) method is developed, which usually relies on the color changes produced by enzymatic reactions as the signal output and has been widely applied to detect pathogens.[7,8] However, the conventional ELISA suffers from insufficient sensitivity and selectivity. To solve those problems, various rapid techniques have been developed for bacterial detection, such as polymerase chain reaction (PCR),[9−12] electrochemical biosensors,[13,14] gene microarrays,[15] and surface plasmon resonance (SPR).[16,17] Among these techniques, polymerase chain reaction (PCR) has been explored as a promising strategy for quantitative, effective, and simultaneous detection of bacteria where it is typically performed in combination with separation techniques.[18−21] But this technique is still time-consuming and has a complicated operation process. Therefore, a detection method that is sensitive, robust, and easy to use and has high sensitivity is still in demand.

Brownian motion is a self-driving capability of microscopic particles generated from random colloidal movement. According to the Stokes−Einstein−Debye relation, the diffusivity is inversely proportional to the viscosity of the fluid when the ambient temperature of the medium and the particle diameter are well controlled.[22,23] Diffusometric methods have been developed in the past for detecting DNA microviscosity,[24] microscale temperature,[25] pathogenic bacteria,[26] and biological targets.[27] Our previous works successfully demonstrated translational Brownian motion as a suitable tool for various biosensing applications.[28−33] However, in comparison with translational Brownian motion, rotational diffusometry (RD)

Received: July 29, 2021
Accepted: September 30, 2021

ACS Publications © XXXX American Chemical Society

shows higher sensitivity and hence provides an effective alternative to trace biomolecule detection.[22,34] An RD technique has been developed and also proven a powerful and highly sensitive analytical tool for various applications such as microvolume viscosity measurement and trace biomolecule detection in our previous works.[34,35] In this study, we use RD to measure the change in viscosity of the fluid in the presence and absence of DNA in the solution. In the presence of DNA, the increased fluid viscosity will result in a lower Brownian motion and the blinking signal of the particles compared to the same fluid without any DNA. This decrease in the blinking signal can be captured and calculated using an in-house cross-correlation algorithm. Janus particles were used in this work by coating a thin gold film on the half-side surface of 1 μm fluorescent polystyrene microbeads. Consecutive blinking images of the modified microbeads were captured at 10 Hz by a CCD camera for 30 s and followed by the application of the cross-correlation algorithm analysis to evaluate the degree of rotational diffusion. A change in correlation time was observed, with the change in the viscosity of the solution serving as a quantitative index of the rotational Brownian motion, which was obtained from the exponential curve fitting of the time-dependent correlation intensity.[36]

In the present work, we focus on determining how PCR-amplified DNA with different thermal cycles, amplicon sizes, and template DNA concentrations affect the viscosity of the solution by using a novel and unconventional biosensing method called rotational diffusometry (RD) and using this technique for the detection of *E. coli*. We also perform a detailed comparison of RD with the conventional PCR and represent the data in the form of maps. These studies provide insight into the rapid and sensitive detection of the pathogen by DNA amplification using RD and propose an integration of this biosensing method in early disease diagnosis in the future.

MATERIALS AND METHODS

Bacterial Culture Growth and Genomic DNA Extraction. Four bacterial strains, including *E. coli* (ATCC 25922), *Staphylococcus aureus* (ATCC 23360), *Listeria monocytogenes* (ATCC 19115), and *Klebsiella pneumoniae* (ATCC 700603), were purchased from American Type Culture Collection (Manassas, VA, USA), and their frozen stocks (20% glycerol and 5 mL of TS broth) were used for the culture preparation. The bacterial culture was grown in TS broth (TSB; 211825, BD, Sparks, MD, USA) at 37 °C for 24 h. Genomic DNA from the prepared bacterial culture was extracted and purified by using a commercially available Gene Spin genomic DNA extraction kit (PT-GD112, Pro-Tech chemicals, Taiwan). Extraction of genomic DNA from *E. coli* and *K. pneumoniae* was performed according to the manufacturer's instructions for the isolation of genomic DNA from Gram-negative bacterial cultures, and in the case of *S. aureus* and *L. monocytogenes*, the extraction was performed according to the manufacturer's instructions for the isolation of genomic DNA from Gram-positive bacterial cultures. The genomic DNA concentration of each bacterial strain was determined using a microvolume UV−Vis spectrophotometer (One Drop Touch Pro, Biometrics Technologies, USA). These extracted DNA samples were used as a template for PCR.

PCR Amplification of the Bacterial DNA. PCR reactions (T100 thermal cycler, Bio-Rad, USA) were performed with isolated genomic DNA using Fast-Run TM 2X Taq Master Mix without dye (PT-TMM228-D, Pro-Tech Chemicals, Taiwan). Primers with different amplicon sizes of 84, 147, and 246 bp (Table 1) for the targeted *uidA* gene of *E. coli* were chosen from the literature.[37−39] Primers were synthesized by Pro-Tech Chemicals, Taiwan. All samples were made in triplicate for testing. A 50 μL single PCR reaction system was set up as mentioned in the literature.[39] All PCR reactions were performed with an initial denaturing step at 95 °C for 4 min, followed by 30 cycles of denaturation at 95 °C for 30 s, annealing at 55 °C for 40 s, extension at 72 °C for 40 s, and a final extension at 72 °C for 10 min. Amplification was confirmed by 1.5% agarose gel electrophoresis using a clear vision DNA stain (PT-D1001, Pro-Tech Chemicals, Taiwan).

Table 1. Primer Sequences for the Target Genes

gene	primer sequence	amplicon length
uidA	forward primer: 5′-CGGAAGCAACGCGTAAACTC-3′	84 bp
	reverse primer: 5′-TGATGGTATCGGTGTGAGCG-3′	
	forward primer: 5′-AAAAC GGCAA GAAAA AGCAG-3′	147 bp
	reverse primer: 5′-ACGCGTGGTTACAGTCTTGCG-3′	
	forward primer: 5′-TGGCT TTGGT CGTCA T-3′	246 bp
	reverse primer: 5′-TCTTT CGGCT TGTTG C-3′	

Theoretical Background of Rotational Diffusometry and Relationship with Viscosity. Brownian motion is defined as the random movement of a microscopic particle in suspension and can be classified into rotational Brownian motion and translational Brownian motion. The rotational diffusivity defined by the Stokes−Einstein−Debye relation mentioned in eq 1[22] is written as:

$$D_r = \frac{K_B T}{\pi \mu d_p^3} \tag{1}$$

where K_B is the Boltzmann constant, T is the absolute temperature, μ is the liquid viscosity, and d_p represents the bead diameter. According to eq 1, the rotational Brownian motion was inversely proportional to the viscosity under the same temperature and particle diameter. Janus microbeads were used to calculate rotational Brownian motion, where these particles were used to generate the blinking signal. Here, we used a cross-correlation algorithm for the measurement of the blinking signals, instead of tracking single particles. The correlation intensity was calculated from the comparison of a series of particle images within a time interval of Δt. The cross-correlation intensity was equivalent to the peak value of the cross-correlation function. With the increase in time interval, the peak value was decreased. The intensity diagram was then normalized from the following exponential regression:

$$A \exp\left(-\frac{t}{\text{Ø}}\right) + B \tag{2}$$

where A and B are constants determined by fitting the exponential curve with data, t is the elapsed time, and Ø is the characteristic correlation time of this curve. Correlation time represents the exponential decay of the initially oriented population of particles. From the Stokes−Einstein−Debye equation, the correlation time can be expressed as:

https://doi.org/10.1021/acs.analchem.1c03209
Anal. Chem. XXXX, XXX, XXX−XXX

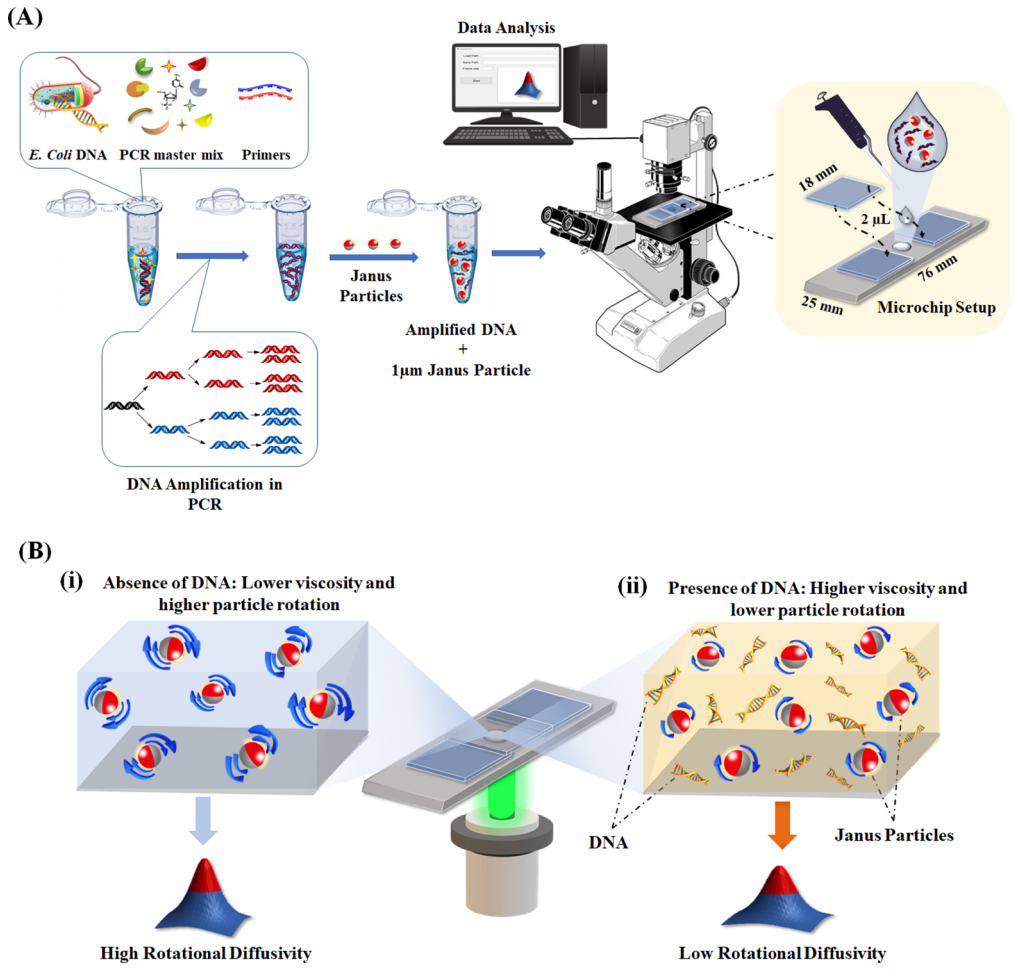

Figure 1. (A) Schematic illustration of the rotational diffusometry experimental setup. PCR amplification of *E. coli* DNA was performed by mixing the appropriate concentration of selected primers, PCR components, and template DNA. A sample containing amplified DNA was mixed with Janus particles, and then a total of 2 μL of the sample suspension was pipetted on the glass slide. The 10× objective lens was used to observe the Janus particles under the IX71 microscope. The images captured by the CCD camera were then calculated in MATLAB software. (B) Illustration of rotational diffusometry (RD) in a microfluidic device with modified Janus particles. (i) In the absence of DNA, the Janus particles show higher rotational Brownian motion with a faster blinking signal. (ii) In the presence of DNA, the solution viscosity increases, which leads to a lower rotational Brownian motion of the particles and slower blinking signals.

$$\emptyset = \frac{\mu V}{K_B T} \tag{3}$$

where V represents the equivalent volume of the microbead, μ represents the fluid viscosity, T is the absolute temperature, and K_B is the Boltzmann constant. Therefore, with a fixed microbead volume and absolute temperature, the exponential decay of particles is directly proportional to the fluid viscosity.

Janus Particle Fabrication. Preparation of uniformly dispersed Janus particles was performed by following the physical deposition method.[40,41] Fluorescent polystyrene particles (1 μm) were purchased from Thermo Fisher Scientific (F13083, Waltham, MA, USA). The surface modification of the clean glass slide was performed by using UV light (wavelength: 172 nm; Hamamatsu Flat Excimer, EX-mini) to make the slide superhydrophilic and then followed by a uniform layer formation of the diluted particle solution on it (0.1% solids in the ethanol). A monolayer of particles was obtained on the glass slide after drying out the suspension for 45 min. A 15 nm thin layer of gold was deposited on the monolayer particles by an e-beam evaporator, with a coating rate of 1 Å/s. The Janus particles were harvested from the glass slide through sonication for 1 h and transferred to the water solution with 1% (v/v) Tween 20 (P1379, Sigma Aldrich). Purification of the Janus particle suspension was performed by filter disk (pore sizes: 5.0 μm) (Membrane Solutions, USA) to remove the aggregated particles and suspended gold fragments. Finally, the suspension was concentrated to 2×10^9 particles/mL by centrifugation, and the final suspension was stored at 4 °C.

Experimental Setup. Janus microbeads (1 μm) were thoroughly mixed with the DNA solution in advance. Sonication (20 s) was performed to ensure thorough dispersion of the microbeads. Exactly 2 μL of the suspension was pipetted onto a glass slide. A glass cover was then placed on top of the suspension droplet with a spacer of 110 μm. By positioning the sandwiched suspension droplet under a fluorescence microscope (IX71, Olympus, Tokyo, Japan) with a 10× objective, a series of consecutive particle images were captured by a CCD camera (Firefly MV FMVU-13S2C, Point Grey, Richmond, BC, Canada) at a frame rate of 10 Hz (Figure 1). Blinking signals measured from the Janus microbeads provided visual information of rotational Brownian motion. Particle images were processed and auto- and cross-correlation analysis was performed using an in-house MATLAB code. Six measurements

https://doi.org/10.1021/acs.analchem.1c03209
Anal. Chem. XXXX, XXX, XXX−XXX

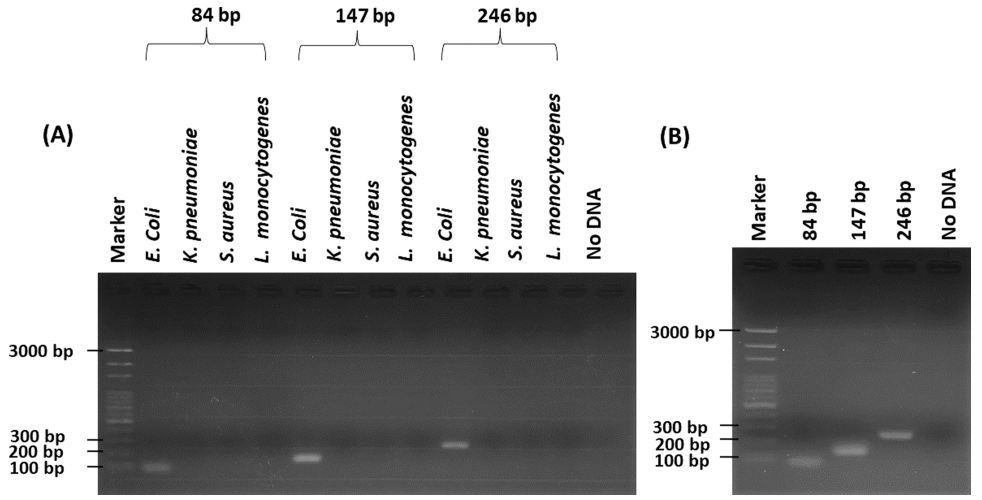

Figure 2. (A) *E. coli* DNA amplification of three different amplicons (84, 147, and 246 bp) for *uidA* gene and their comparison with various control strains. (B) *E. coli* DNA amplification of three different amplicons (84, 147, and 246 bp) for *uidA* gene from the mixture of *E. coli* and three control strain DNA.

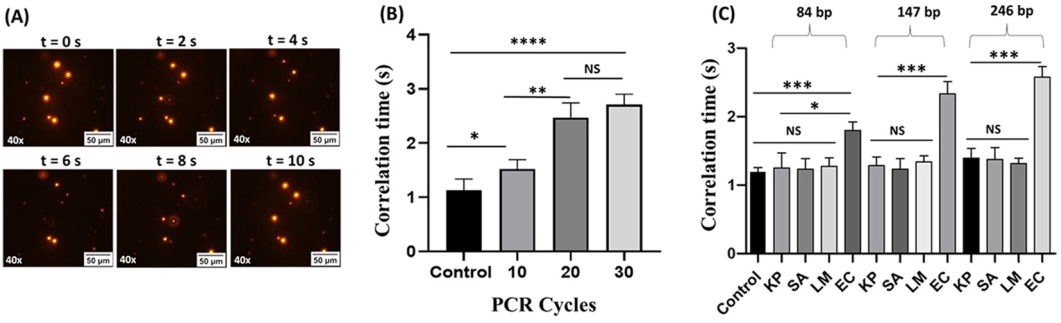

Figure 3. (A) Image sequence of 1 μm Janus particles under a fluorescence microscope (40×). (B) Change in correlation time with respect to various thermal cycles (amplicon size, 246 bp). (C) Change in correlation time of three different amplicons (84, 147, and 246 bp) for *uidA* gene and their comparison with various control strains at 30 thermal cycles (EC, *E. coli*; SA, *S. aureus*; LM, *L. monocytogenes*; KP, *K. pneumoniae*) (*$p < 0.05$, **$p < 0.01$, ***$p < 0.001$, and ****$p < 0.0001$; $n = 3$).

of 300 images each were performed for every sample, and the characteristic correlation times were plotted.

RESULTS AND DISCUSSION

Organism Specific Gene Selection and Specificity Studies. The *uidA* gene of *E. coli* was evaluated in this study, and the optimized PCR conditions were followed according to the literature.[39] The primer pairs of three different amplicon sizes of 84, 147, and 246 bp were selected in this study. The amplified target DNA fragments of the bacteria were initially identified by 1.5% agarose gel electrophoresis. The selectivity of the chosen primers was tested with *K. pneumoniae*, *S. aureus*, and *L. monocytogenes*, and the DNA templates were extracted from each bacterium and then adjusted to the same concentration. No other peaks were observed in the PCR products apart from *E. coli*, confirming the selectivity of the primers (Figure 2A). To further test the specificity of the primers, we mixed the genomic DNA of all the four bacterial species and performed PCR. No other nonspecific amplification was observed in the gel image, signifying the specificity of the primers (Figure 2B).

Detection of *E. coli* DNA Amplification Using Rotational Diffusometry (RD). Rotational diffusometry (RD) was applied for the detection of *E. coli* DNA amplification, where 1 μm modified Janus particles were incubated in the PCR-amplified DNA solution. The characterization of Janus particles is well explained in our previous work.[34] The experimental temperature of the microchips was maintained at 25 °C for all experiments. Six droplets were placed on a microchip at a distance of 200 μm apart. Images of blinking particles were recorded for each concentration followed by analysis using an in-house cross-correlation algorithm (Figure 3A). The change in the correlation time indicates the viscosity change in the solution, confirming the amplification of *E. coli* DNA (Figure 3). All PCR amplification was also examined and confirmed by gel electrophoresis (Figures S1 and S3, Supporting Information). Figure 3B,C shows a relatively statistically significant difference ($p < 0.0001$, $n = 3$) in the correlation time between the particles suspended in the PCR-amplified DNA sample in comparison to the control group, which has undergone the thermal cycles containing all PCR components, except the template DNA, indicating a successful detection of *E. coli* DNA amplification by rotational diffusometry.

For a better understanding, we have performed the experiments with different thermal cycles while fixing the amplicon size for 246 bp. Figure 3B shows a significant difference of relative correlation time between the control group and the DNA amplified with 10 cycles, indicating a rapid detection of *E. coli*, while in the case of conventional PCR, it is detectable only up to 20 cycles (Figure S1). No significant difference was observed between the sample containing amplified DNA with 20

https://doi.org/10.1021/acs.analchem.1c03209
Anal. Chem. XXXX, XXX, XXX−XXX

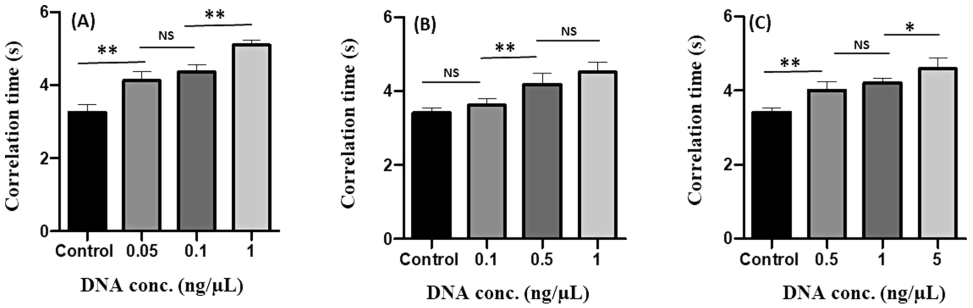

Figure 4. Correlation time plot of PCR-amplified DNA of *E. coli* with respect to the template DNA concentration for an 84 bp amplicon: (A) 30 PCR cycles, (B) 20 PCR cycles, and (C) 10 PCR cycles (*$p < 0.05$, **$p < 0.01$; $n = 3$).

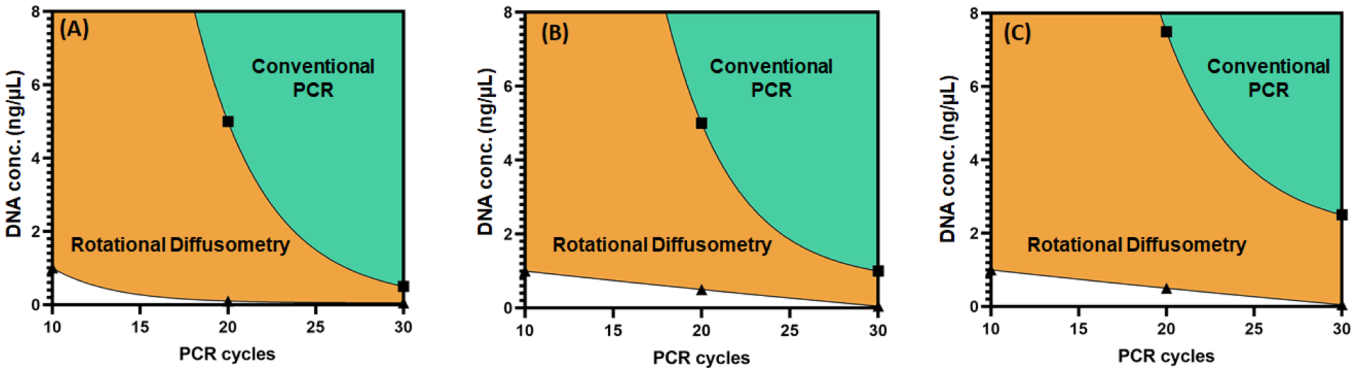

Figure 5. Maps of conventional PCR vs rotational diffusometry for the detection of *E. coli* with respect to template DNA concentration and PCR cycles. The orange part represents the area of rotational diffusometry and the green part represents the area of conventional PCR for the detection of *E. coli*. (A) Plot for template DNA concentration with the function of PCR cycles for a 246 bp amplicon. (B) Plot for template DNA concentration with the function of PCR cycles for a 146 bp amplicon. (C) Plot for template DNA concentration with the function of PCR cycles for an 84 bp amplicon.

and 30 cycles, which is probably due to the less difference in the amount of amplified DNA, causing less viscosity change. In another study, we wanted to check the effect of the amplicon size on RD measurement with a fixed thermal cycle. For that, we have chosen three different primer pairs of different amplicon sizes, *viz.*, 84, 147, and 246 bp, and 30 thermal cycles have been run for this study. All the primers were also tested with three control strains, *viz.*, *K. pneumoniae*, *S. aureus*, and *L. monocytogenes*. No statistically significant difference was found between the control (without any genomic DNA) and the samples containing DNA of the control strains (Figure 3C). However, a gradual increase in the correlation time was noticed with the increase in amplicon length for the sample containing *E. coli* genomic DNA (Figure 3C). No statistically significant difference was observed in the RD measurements among the amplified samples with different amplicons, while a significant difference was noticed ($p < 0.05$, $n = 3$) between the samples of 84 and 246 bp amplicons. This indicates that the size difference between the amplified products was too small to identify a significant difference in viscosity; however, it was noteworthy to mention that successful identification of *E. coli* DNA amplification with different lengths of amplicons is still possible using this method.

Effect of DNA Concentration on *E. coli* Detection. The concentration of the template DNA plays an important role in detection methods based on nucleic acid amplification. After evaluating the rotational diffusometry for the successful detection of *E. coli* DNA amplification, we moved our focus to study the effect of concentration of template DNA on *E. coli* detection using RD and compare it with conventional PCR. Therefore, we performed a series of experiments with different concentrations of *E. coli* genomic DNA with respect to different thermal cycles and the amplicon length (Figure 4). A statistically significant higher correlation time was observed (Figure 4A) compared to control ($p < 0.01$, $n = 3$), where the detection of *E. coli* was achieved with 50 pg/μL genomic DNA using the RD method for 30 thermal cycles. However, in the case of the conventional method, it was detectable only up to 2.5 ng/μL (Figure S3a). Additionally, the detection sensitivity of 500 pg/μL was achieved for 10 thermal cycles with a statistically significant difference in values ($p < 0.01$, $n = 3$) between the control and the amplified sample for RD (Figure 4C), where no signal was distinguished for conventional PCR (Figure S3). This indicates the higher sensitivity of RD even for very low thermal cycles. RD measurement data for 147 and 246 bp amplicons are displayed in Figure S2 (all the gel images are shown in Figure S3, Supporting Information,).

For an easy and better understanding, we demonstrated our findings in Figure 5 in the form of maps that represent the comparison between the RD and conventional PCR for the detection of *E. coli*. The data points of each map resemble the detection of *E. coli* for each method concerning DNA concentration and PCR cycles, dividing the maps into three different regions. It was perceivable from Figure 5 that RD has much higher detection sensitivity compared to conventional PCR. While conventional PCR can detect only up to 20 thermal cycles, using RD, *E. coli* is detectable up to 10 thermal cycles. However, RD is much more efficient and sensitive in the lower thermal cycles, as the detection gap between RD and conventional PCR drastically increases and reaches the plateau at 10 cycles. Using rotational diffusometry, the DNA amplification is detectable for 10 thermal cycles, and the overall turnaround time for this technique appears to be less than 60

https://doi.org/10.1021/acs.analchem.1c03209
Anal. Chem. XXXX, XXX, XXX−XXX

min, where 50 min is required for thermal cycling and 1 min for particle mixing with the amplified DNA sample, followed by 30 s of image capturing and 5 min of data analysis. Compared with conventional PCR, this technique appears to improve the overall measurement time by 2.5-fold by reducing the thermal cycle numbers from 20 to 10 as well as the entire gel electrophoresis step. Furthermore, the detection gap between RD and conventional PCR is inversely proportional to the size of amplicons, demonstrating the better sensitivity of RD for *E. coli* detection with shorter-sized genes. One more significant use of this map is it provides detailed information and helps identify the use of the suitable method for *E. coli* detection with respect to different thermal cycles and concentrations of genomic DNA. This study delivers a distinct conclusion that RD is an efficient, fast, and sensitive method for the detection of nucleic acid amplification.

CONCLUSIONS

In this study, we demonstrated that rotational diffusometry could be a unique tool for early and sensitive detection of *E. coli*. We compared RD with conventional PCR, and our studies represent RD as an alternative solution for rapid and selective detection of pathogenic bacteria. Detection sensitivity is achieved in this platform with 50 pg/μL of *E. coli* genomic DNA with a measurement time of 30 s and a sample volume of 2 μL. The turnaround time for *E. coli* detection by RD was less than 60 min. Other studies showed a successful identification of DNA amplification up to 10 thermal cycles with different sizes of amplicons. Additionally, three maps provide a clear comparison between conventional PCR and RD for the detection of *E. coli*, and from these maps, one can easily identify the suitable method to be used for *E. coli* detection with respect to DNA concentration and various thermal cycles. Our findings demonstrated that RD is a definitive method for the detection of nucleic acid amplification and has a broad-spectrum application in microorganism detections. This method can also overcome the limitations of real-time PCR like long analysis time (4−6 h) and high-tech instrument dependence, and we look forward to advancing this method further to provide a laboratory workflow for robust, sensitive, and selective detection of pathogens.

ASSOCIATED CONTENT

Supporting Information

The Supporting Information is available free of charge at https://pubs.acs.org/doi/10.1021/acs.analchem.1c03209.

Rotational diffusometry data, gel electrophoresis images, milk sample analysis, and bacterial detection range in clinical samples (PDF)

Comparison of particle rotation in control and a sample containing PCR-amplified DNA (MP4)

AUTHOR INFORMATION

Corresponding Author

Han-Sheng Chuang − *Department of Biomedical Engineering and Medical Device Innovation Center, National Cheng Kung University, Tainan 701, Taiwan;* orcid.org/0000-0002-7257-6565; Email: oswaldchuang@mail.ncku.edu.tw

Authors

Dhrubajyoti Das − *Department of Biomedical Engineering, National Cheng Kung University, Tainan 701, Taiwan*

Wei-Long Chen − *Department of Biomedical Engineering, National Cheng Kung University, Tainan 701, Taiwan*

Complete contact information is available at: https://pubs.acs.org/10.1021/acs.analchem.1c03209

Notes

The authors declare no competing financial interest.

ACKNOWLEDGMENTS

This research work was supported by Ministry of Science and Technology (MOST), Taiwan, project numbers 108-2628-E-006-002-MY3 and 109-2811-E-006-535.

REFERENCES

(1) Cheng, N.; Song, Y.; Zeinhom, M. M. A.; Chang, Y.-C.; Sheng, L.; Li, H.; Du, D.; Li, L.; Zhu, M.-J.; Luo, Y.; Xu, W.; Lin, Y. *ACS Appl. Mater. Interfaces* **2017**, *9*, 40671−40680.

(2) Hall-Stoodley, L.; Costerton, J. W.; Stoodley, P. *Nat. Rev. Microbiol.* **2004**, *2*, 95−108.

(3) Malorny, B.; Paccassoni, E.; Fach, P.; Bunge, C.; Martin, A.; Helmuth, R. *Appl. Environ. Microbiol.* **2004**, *70*, 7046−7052.

(4) Zheng, L.; Cai, G.; Wang, S.; Liao, M.; Li, Y.; Lin, J. *Biosens. Bioelectron.* **2019**, *124*−*125*, 143−149.

(5) Velusamy, V.; Arshak, K.; Korostynska, O.; Oliwa, K.; Adley, C. *Biotechnol. Adv.* **2010**, *28*, 232−254.

(6) Huang, F.; Zhang, H.; Wang, L.; Lai, W.; Lin, J. *Biosens. Bioelectron.* **2018**, *100*, 583−590.

(7) Zhao, Y.; Zeng, D.; Yan, C.; Chen, W.; Ren, J.; Jiang, Y.; Jiang, L.; Xue, F.; Ji, D.; Tang, F.; Zhou, M.; Dai, J. *Analyst* **2020**, *145*, 3106−3115.

(8) Shen, Z.; Hou, N.; Jin, M.; Qiu, Z.; Wang, J.; Zhang, B.; Wang, X.; Wang, J.; Zhou, D.; Li, J. *Gut Pathog.* **2014**, *6*, 14.

(9) Fratamico, P. M.; Bagi, L. K.; Pepe, T. *J. Food Prot.* **2000**, *63*, 1032−1037.

(10) Liang, T.; Wu, X.; Chen, B.; Liu, J.; Aguilar, Z. P.; Xu, H. *LWT* **2020**, *130*, 109642.

(11) Du, J.; Wu, S.; Niu, L.; Li, J.; Zhao, D.; Bai, Y. *Anal. Methods* **2020**, *12*, 212−217.

(12) Deshmukh, R. A.; Bhand, S.; Roy, U. *Anal. Methods* **2019**, *11*, 3155−3167.

(13) Brandão, D.; Liébana, S.; Campoy, S.; Cortés, M. P.; Alegret, S.; Pividori, M. I. *Biosens. Bioelectron.* **2015**, *74*, 652−659.

(14) Cesewski, E.; Johnson, B. N. *Biosens. Bioelectron.* **2020**, *159*, 112214.

(15) Straub, T. M.; Dockendorff, B. P.; Quiñonez-Díaz, M. D.; Valdez, C. O.; Shutthanandan, J. I.; Tarasevich, B. J.; Grate, J. W.; Bruckner-Lea, C. J. *J. Microbiol. Methods* **2005**, *62*, 303−316.

(16) Wang, Y.; Knoll, W.; Dostalek, J. *Anal. Chem.* **2012**, *84*, 8345−8350.

(17) Lee, N.; Choi, S.-W.; Chang, H.-J.; Chun, H. S. *J. Food Prot.* **2018**, *81*, 713−718.

(18) Li, Y.; Zhuang, S.; Mustapha, A. *Meat Sci.* **2005**, *71*, 402−406.

(19) Fabiani, L.; Pucci, E.; Delibato, E.; Volpe, G.; Piermarini, S.; De Medici, D.; Capuano, F.; Palleschi, G. *Talanta* **2017**, *166*, 321−327.

(20) Wang, L.; Li, Y.; Mustaphai, A. *J. Food Prot.* **2007**, *70*, 1366−1372.

(21) Agarwal, A.; Makker, A.; Goel, S. K. *Mol. Cell. Probes* **2002**, *16*, 243−250.

(22) Debye, P. *J. Soc. Chem. Ind.* **1929**, *48*, 1036−1037.

(23) Miller, C. C. *Proc. R. Soc. London, Ser. A* **1924**, *106*, 724−749.

(24) Clayton, K. N.; Berglund, G. D.; Linnes, J. C.; Kinzer-Ursem, T. L.; Wereley, S. T. *Anal. Chem.* **2017**, *89*, 13334−13341.

(25) Mayor, P.; D'Anna, G.; Barrat, A.; Loreto, V. *New J. Phys.* **2005**, *7*, 28.

(26) Moehling, T. J.; Lee, D. H.; Henderson, M. E.; McDonald, M. K.; Tsang, P. H.; Kaakeh, S.; Kim, E. S.; Wereley, S. T.; Kinzer-Ursem, T. L.; Clayton, K. N.; Linnes, J. C. *Biosens. Bioelectron.* **2020**, *167*, 112497.

(27) Clayton, K. N.; Lee, D.; Wereley, S. T.; Kinzer-Ursem, T. L. *Lab Chip* **2017**, *17*, 4148−4159.
(28) Wang, J.-C.; Tung, Y.-C.; Ichiki, K.; Sakamoto, H.; Yang, T.-H.; Suye, S.; Chuang, H.-S. *Biosens. Bioelectron.* **2020**, *148*, 111817.
(29) Cheng, H.-P.; Chuang, H.-S. *ACS Sens.* **2019**, *4*, 1754−1760.
(30) Yang, Y.-T.; Wang, J.-C.; Chuang, H.-S. *Biosensors* **2020**, *10*, 181.
(31) Chuang, H.-S.; Chen, Y.-J.; Cheng, H.-P. *Biosens. Bioelectron.* **2018**, *101*, 75−83.
(32) Wang, J.-C.; Chi, S.-W.; Yang, T.-H.; Chuang, H.-S. *ACS Sens.* **2018**, *3*, 2182−2190.
(33) Wang, J.-C.; Chi, S.-W.; Shieh, D.-B.; Chuang, H.-S. *Sens. Actuators, B* **2019**, *278*, 140−146.
(34) Chen, W.-L.; Chuang, H.-S. *Anal. Chem.* **2020**, *92*, 12996−13003.
(35) Chen, C.-J.; Chen, W.-L.; Phong, P. H.; Chuang, H.-S. *Sensors* **2019**, *19*, 1271.
(36) Lavalette, D.; Tétreau, C.; Tourbez, M.; Blouquit, Y. *Biophys. J.* **1999**, *76*, 2744−2751.
(37) Zhang, Y.; Zhu, L.; Zhang, Y.; He, P.; Wang, Q. *J. Chromatogr. A* **2018**, *1555*, 100−105.
(38) Miotto, M.; Fonseca, A. A. J.; Barretta, C.; da Silva, H. S.; Pellizzaro, T.; De Dea Lindner, J.; Vieira, C. R. W.; Parveen, S.; Prudencio, E. S. *Food Microbiol.* **2019**, *77*, 85−92.
(39) Zhang, Y.; Hu, X.; Wang, Q. *Microchem. J.* **2020**, *157*, 104876.
(40) Love, J. C.; Gates, B. D.; Wolfe, D. B.; Paul, K. E.; Whitesides, G. M. *Nano Lett.* **2002**, *2*, 891−894.
(41) Takei, H.; Shimizu, N. *Langmuir* **1997**, *13*, 1865−1868.

https://doi.org/10.1021/acs.analchem.1c03209
Anal. Chem. XXXX, XXX, XXX−XXX